OXFORD

SOT | Society of Toxicology
www.toxsci.oxfordjournals.org

*TOXICOLOGICAL SCIENCES*, 156(2), 2017, 336–343

doi: 10.1093/toxsci/kfw258
Advance Access Publication Date: December 20, 2016
Research article

# ZnO Nanoparticles Enhanced Germ Cell Apoptosis in *Caenorhabditis elegans*, in Comparison with $ZnCl_2$

Brittany O'Donnell,[*,†,1] Lily Huo,[‡,1] Joseph R. Polli,[§] Li Qiu,[¶] David N. Collier,[‖] Baohong Zhang,[*] and Xiaoping Pan[*,2]

[*]Department of Biology, East Carolina University, Greenville, North Carolina; [†]West Pharmaceutical Services, Inc. Kinston, North Carolina 28504; [‡]Junius H Rose High School, Greenville, North Carolina 27858; §Department of Pharmaceutical Sciences, SUNY-Buffalo, New York, 14260; ¶College of Veterinary Medicine, Northwest Agriculture and Forestry University, Yangling 712100, China; and ‖Department of Pediatrics, East Carolina University, Greenville, North Carolina 27858

[1]These authors contributed equally to this study.
[2]To whom correspondence should be addressed at Department of Biology, East Carolina University N108 Howell Science Complex, Greenville, NC 27858. Fax: +1 252 328 4718. E-mail: panx@ecu.edu or xppan23@gmail.com.

## ABSTRACT

Effects of ZnO NPs and ionic Zn on germline apoptosis and the regulation of genes in the apoptosis pathway were investigated in vivo using the model organism *Caenorhabditis elegans*.Age synchronized Bristol N2 worms were exposed to ZnO NPs and $ZnCl_2$ at concentrations of $6.14 \times 10^{-1}$, 61.4, and 614 μM form larval stage 1 (L1) to early adulthood. Possible ZnO nanoparticles were observed under the worm cuticle and also in the gonadal region by transmission electron microscopy (TEM). ZnO NPs and $ZnCl_2$ both significantly increased the number of apoptotic cells as compared with controls in the 61.4 and 614 μM treatment groups ($P < .05$). However, ZnO NPs induced more apoptotic cells in the 61.4 μM treatment than $ZnCl_2$ ($P < .05$), suggesting ZnO NP is more potent in inducing apoptosis at specific exposure concentration. Findings using the MD701 (*bcIs39 [(lim-7)ced-1p::GFP + lin-15(+)]*) strain further confirmed the observations in N2 strain. Genes involved in the apoptosis pathway (*ced-13, ced-3, ced-4, ced-9, cep-1, dpl-1, efl-1, efl-2, egl-1, egl-38, lin-35, pax-2*, and *sir-2.1*) were in general upregulated in response to ZnO NP exposure. The *cep-1*/p53 gene was up-regulated in gene expression assay. In the *cep-1* loss of function mutant, no significant increase in apoptosis was observed. Therefore, the increased apoptosis resulting from ZnO NPs exposure is likely *cep-1*/p53 dependent. This study provides evidence that ZnO nanoparticles affect germ cell apoptotic machinery as a potential mechanism of reproductive toxicity.

**Key words:** nanoparticles; ZnO; *C. elegans*; apoptosis; gene expression; cep-1/p53 pathway.

Nanomaterials are produced in metric tons per year and the production is expected to increase over the next decade (Nel *et al.*, 2006; USEPA, 2005). In particular, ZnO NPs are used in products that humans come into contact with on a daily basis such as, toothpaste, sunscreens, cosmetics or beauty products, and textiles (Wang *et al.*, 2009). Due to expected increases of manufactured NPs and the frequency of human contact with NPs, research on biological effects of NPs like ZnO NPs is of importance. Previous studies have used the model organism *Caenorhabditis elegans* to assess effects of manufactured ZnO NPs. Mortality, growth, movement, and reproduction (number of eggs and offspring) were used as toxicity endpoints (Ma *et al.*, 2009; Wang *et al.*, 2009). It was found that ZnO NPs exposure results in inhibition of growth, behaviors, reproduction or increased mortality at various concentrations including environmentally relevant concentrations (Ma *et al.*, 2009; Wang *et al.*, 2009; Wu *et al.*, 2013). Findings suggests the production of reactive oxygen species (ROS) is highly correlated with various ZnO NPs-induced toxicity, since the treatment with antioxidants suppressed various toxic effects (Wu *et al.*, 2013). Studies also suggested that ROS

production and dissolved ionic Zn may not fully explain the toxicity (Ma *et al.*, 2009; Wang *et al.*, 2009).

A significant gap exists in our understanding the mechanism of these ZnO NPs induced adverse effects. *C. elegans* are increasingly used as a model system for toxicological studies for an extensive variety of environmental toxicants (Kaletta and Hengartner, 2006; Leung *et al.*, 2008). The *C. elegans* has a short life cycle (approximately 3 days at 20°), high reproduction capacity (approximately 300 progeny in wide-type hermaphrodites) that allows research on the reproductive effects to be achieved in a relatively short period of time. Its translucent body allows developmental staging and reproductive processes to be monitored by microscopy easily. The *C. elegans* genome has been completely sequenced and has a high level of conservation to higher organisms including humans (Consortium, 1998; Cutter *et al.*, 2009). Especially, the *C. elegans* germ cell apoptosis is a highly conserved process; many genes in the apoptosis pathways are conserved with humans (Hengartner, 1997). During oocyte development, normally 50% of predetermined oocytes undergo apoptosis, and subsequently serve as a population of nurturing cells, providing mature oocytes with cytoplasmic components (Gumienny *et al.*, 1999). Once the nurse cells have been utilized apoptosis is activated producing a nurse cell corpse which is engulfed by neighboring somatic gonad sheath cells (Gumienny *et al.*, 1999). The *C. elegans* germ cell apoptosis can be induced by environmental stressors such as DNA damage and pathogenic infection. Environmental stress can cause a significant increase in apoptosis beyond the normal range for producing nurse cells. Excess apoptosis can reduce the number of mature oocytes and thus reduce the number of offspring (Polli *et al.*, 2014; Ruan *et al.*, 2012).

This study investigated effects of ZnO NPs exposure on *C. elegans* germ cell apoptosis and related gene expressions, proposed as a potential mechanism of observed reproductive inhibition reported by previous studies. Since dissolved ionic Zn may contribute to the toxic effects, we are also interested in comparing the apoptosis-inducing effects of ZnO NPs with $ZnCl_2$.

## MATERIALS AND METHODS

### Materials

ZnO nanopowder was obtained from Sigma-Aldrich, the physiochemical properties provided by the manufacturer is as followings: approximately 80% Zn basis, approximately 100% pure, <100 nm, surface area 15–25 $m^2/g$. Anhydrous $ZnCl_2$ were also purchased from Sigma-Aldrich with a purity of 99.99%.

#### *Size Characterization of ZnO NPs by Transmission Electron Microscopy*

A drop of ZnO NPs (10 ul) at the concentration of 614 μM in ultrapure water solution was placed onto a copper grid and allow the water to evaporate before transmission electron microscopy (TEM) analysis. A FEI CM12 TEM was used for ZnO NP analysis. The images were captured by an AMT XR50 5 megapixel digital camera and then exported to the ImageJ, a free Java-based software package provided by the National Institutes of Health, for particle size analysis. The nanoparticles appeared darker in contract with the background due to its higher electron density as compared with the grid coating material. For spherical, nonspherical or agglomerated particles, the software always measure the diameter of all particles at a fixed angle and convert pixels to length. Given the orientation of the particles is typically random and a large sample size (n = 400) was used, sound results regarding particle sizes and distribution can be generated.

#### *Hydrodynamic Size Characterization of ZnO NPs by Dynamic Light Scattering*

The ZnO nanoparticle at the concentration of 614 μM was suspended in ultrapure water and dispersed by probe sonication (100 W, 40 kHz) for 1 h. A Malvern Zetasizer instrument was used for ZnO nanoparticle size and distribution analysis. A 1 ml of ZnO nanoparticle suspension, was placed into the sizing cuvette, make sure free of bubble, and then subjected to the instrument measurement at room temperature. The default settings of the instrument were adopted for the measurement. The Dynamic Light Scattering (DLS) measurement used by the Zetasizer instrument is a type of spectroscopy technique that uses a laser light source and measure the intensity of light scattered from the ZnO nanoparticle suspension. The mean and standard deviation of the particle size were calculated by using instrument readings of 4 independent measurements.

#### *Imaging of ZnO NPs* In Vivo

N2 worms were dosed with 61.4 and 614 μM ZnO NP that correspond to 4, and 40 mg Zn/l. Both treatments and control. As the "long-term" effects were of interests, worms were dosed from L1 to adult stage for 72 h, spanning the whole life cycle until early adult stage where apoptosis can be visualized. Worms from control and both treatment groups (n = 12 for each group) were fixed and sectioned into 60–90 nm sections, stained and then observed under TEM.

#### C. elegans *Strains and Culture*

Three strains of *C. elegans* were used: wild-type Bristol N2, MD701 (*bcIs39 [(lim-7)ced-1p::GFP + lin-15(+)]*), and TJ1(*cep-1(gk138) I*).The culture of these 3 *C. elegans* strains was according to standard procedure: *Escherichia coli* OP50 was used as the food resource and *C. elegans* were cultured in the nematode growth medium (NGM) agar [19]. Age-synchronization was achieved using a bleach and NaOH solution to collect eggs from gravid worms (Brenner, 1974). Eggs in the M9 buffer solution were then hatched without food and synchronized L1 population was obtained.

Aggregated chromosome of apoptotic cells in the N2 stain worms can be visualized as solid green florescence dots following SYTO12 staining; The MD701 strain also has a wide-type background and allows visualization of apoptotic cells without staining. The *ced-1* gene was tagged with green fluorescent protein (GFP) in MD701 strain and is upregulated when cells undergo apoptosis, serving as a signal to promote the engulfment of cell corpses by phagocytic sheath cells. As CED-1 expresses on the cell membrane, apoptotic cells can be visualized as a green fluorescent circle in the loop region of the *MD701* gonad. The TJ1 strain is a *cep-1* loss of function mutant used to determine if *cep-1* is needed in the ZnO NP-induced apoptosis. The gene *cep-1* in *C. elegans* is a p53 homolog involved in the DNA damage induced apoptosis.

#### *Animal Treatments and Apoptosis Assays*

Agar dosing plates were made by mixing calculated amount of ZnO NPs or $ZnCl_2$ solution into the agar medium to make various concentrations ($6.14 \times 10^{-1}$, 61.4, 614 μM ZnO NP and $ZnCl_2$, which correspond to 0.4, 4, and 40 mg Zn/l for both ZnO and $ZnCl_2$. The dosages were selected as similar to what tested in the previous reports that reproductive toxicity was observed. (Ma *et al.*, 2009; Wang *et al.*, 2009). We are interested in

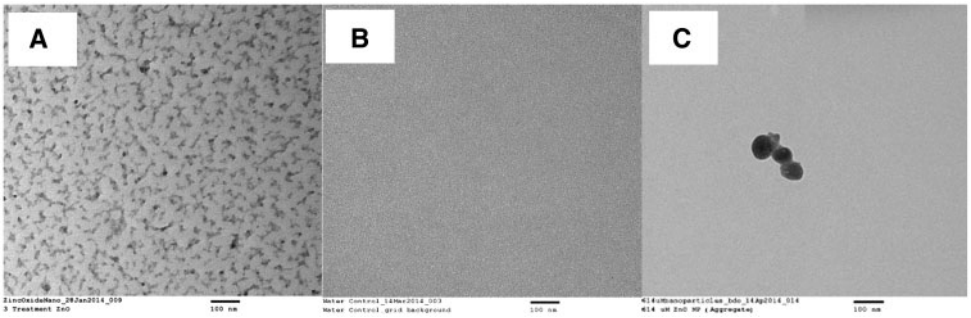


FIG. 1. TEM image of ZnO nanoparticles. **A,** ZnO NPs; **B,** Water control; and **C,** ZnO NPs aggregates observed at higher magnification.

investigating, if germ cell apoptosis also occur and whether germ line apoptosis-related genes are regulated under the similar exposure level. Given the ZnO NPs has been used in many commercial products where human exposure level varies, the dosage tested are also considered human exposure relevant.

Exposure time was from the L1 to the adult stage which last for approximately 72 h at 20°C. The early adulthood were identified as the embryos start appearing. There were 3 biological replicates for each concentration of ZnO NPs and $ZnCl_2$ treatments.

SYTO 12 staining of treated worms and controls was performed following a standard protocol (Gumienny *et al.*, 1999). Briefly, worms were stained with SYTO12 (50 μM) for 1 h in the dark, after staining, worms were washed with PTW (1 × PBS, 0.1% Tween 20), centrifuged and supernatant discarded. Worms were then transferred to fresh NGM agar plates for 1 h to allow the dye to exit intestines. Worms were placed onto 2% agar pads with 5 mM levamisole added to prevent moving. Observation of apoptotic cells in the gonadal loop area were performed under a fluorescence microscope Zeiss Axio Observer Z1. Apoptotic cells were identified? as solid fluorescence dots. The same SYTO 12 staining procedure was performed on the TJ-1 strain too.

The MD701 strain was also used to determine apoptotic cell number under the same treatments as described earlier. Apoptotic cells on MD701 were recorded as bright green florescent circles in the gonadal loop where the programmed cell death occurs. Experiments using the MD701 strain were performed on both ZnO NPs and $ZnCl_2$ treatments for comparison.

### *Total RNA Extraction and Gene Expression Analysis*

Gene expression analysis was performed on worms under the same exposure conditions. After exposure, worms were rinsed with K-medium twice to remove residual bacteria and collected as pellet in a 1.5 ml microcentrifuge tube. The tubes were frozen in liquid nitrogen and then stored in a −80°C freezer until RNA extraction. Total RNA was extracted using mirVanaTM miRNA Isolation Kit (Life Technologies). Quality and purity of extracted RNA was quantified using a Nanodrop ND-1000 (Nanodrop Technologies, Wilmington, Delaware, USA). For reverse transcription (RT), 1000 ng of total RNA from control and each treatment sample were used. RNA was reverse transcribed to single-stranded cDNA using the reverse primer PolyT. Each reaction contained a calculated amount of reagents: DNase/RNase-free water, 1000 ng of total RNA, 0.19 μl RNase Inhibitor (20 U/μl), 0.15 μl 100 mM dNTPs, 10× RT Buffer, 1 μl MultiScribeTM Reverse Transcriptase (50 U/μl), and 2 μl of Poly(T) Primer Mix.

The expressions of thirteen genes (*ced-13, ced-3, ced-4, ced-9, cep-1, dpl-1, efl-1, efl-2, egl-1, egl-38, lin-35, pax-2,* and *sir-2.1*) in the germline apoptosis pathway were tested. Quantitative real-time PCR (qRT-PCR) reactions were performed using a ViiATM 7 Real-Time PCR, each reaction contains: 5.5 μl DNase/RNase free water, 7.5 μl SYBR green PCR Master Mix, 1 μl RT PCR product (diluted with 85 μl of DNase/RNase free water), and 1 μl of primer mix. The System program is as followings: polymerase activation stage of 95 °C for 10 min, followed by 40 cycles of 95 °C for 15 s, and a final stage for annealing and elongation at 60 °C for 60 s. Four biological replicates were performed per treatment group with each having 3 technical replicates. The gene Y45F10D.4, coding for an iron-sulfur binding protein, was used as a reference gene for qRT-PCR results normalization. The ΔΔCt method was used to determine the gene expression fold changes compared with control (Livak and Schmittgen, 2001).

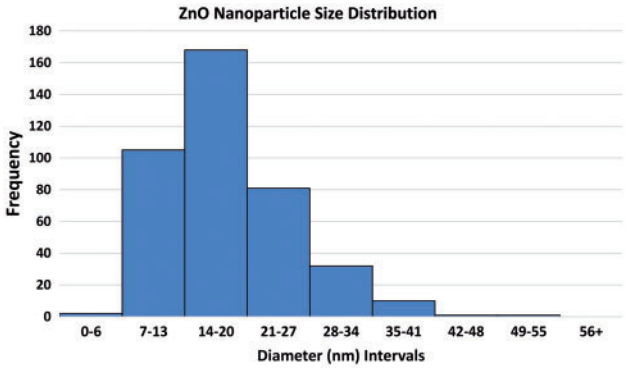


FIG. 2. Frequency histogram of ZnO nanoparticle size distribution determined by TEM.

### *Data Analysis*

The IBM SPSS Statistics 22 software was used for statistical analysis. The statistical test analysis of variance (ANOVA) was used to determine if there was a difference in apoptosis cell counts and gene expression fold changes between treatments groups and the control. If there was a significant difference among treatment groups at $P < .05$ level, least significant difference multiple comparisons were conducted to compare means among groups.

## RESULTS

### *Size Characterization of ZnO NPs*

The sizes of ZnO NPs were firstly determined by TEM (Figure 1). The average size was 17.9 ± 7.3 nm with a distribution range of 1–55 nm. Most ZnO NPs are in 7–34 nm (Figure 2). The hydrodynamic diameter of the ZnO nanoparticles determined by a Malvern Zetasizer was 721 ± 109.5 nm (n = 4).

### *Potential ZnO Nanoparticles* In Vivo

Figure 3 shows the representative images of possible nanoparticles found in the gonadal region (Figure 3A) and also under the

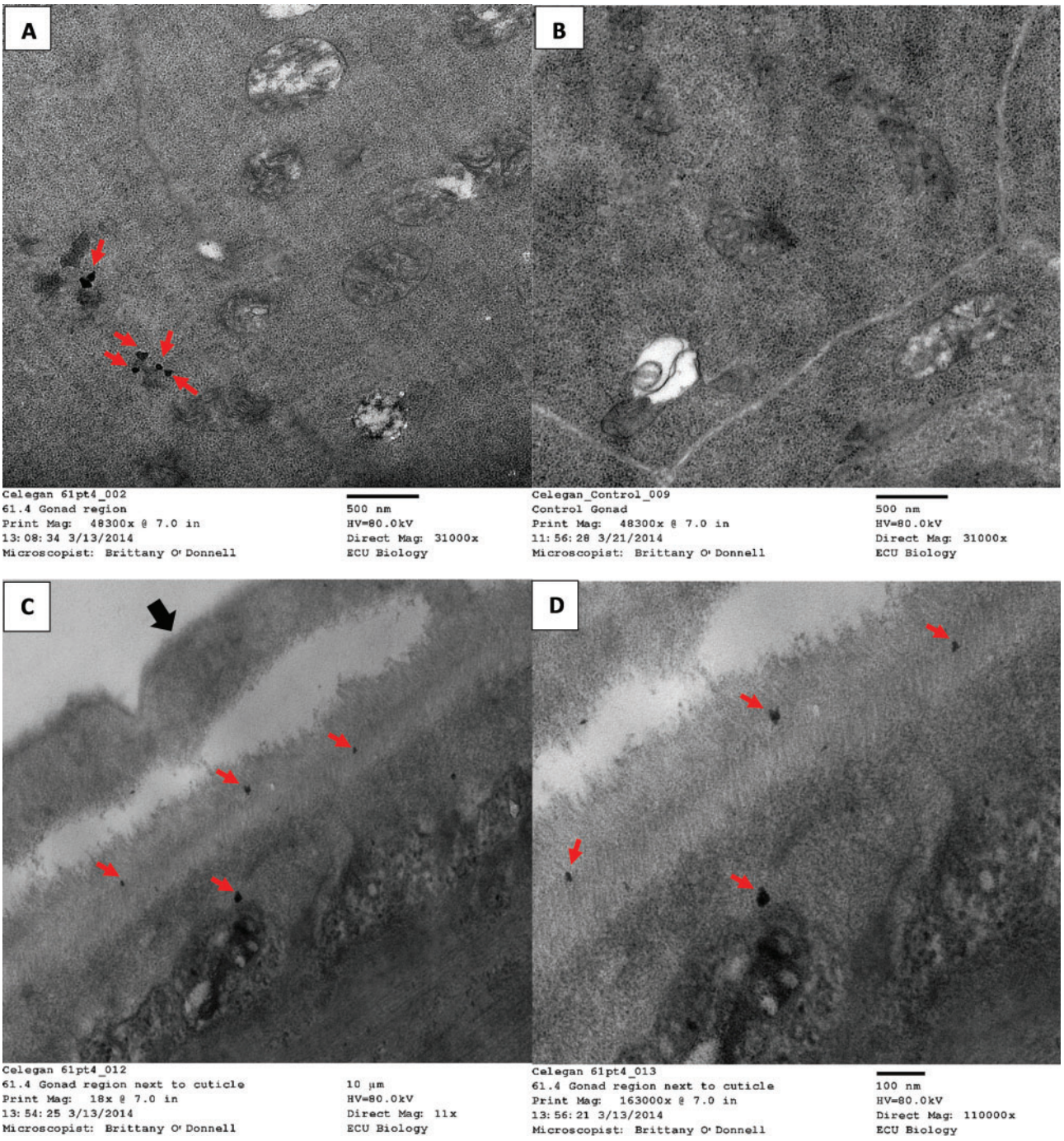


FIG. 3. A, TEM image of possible nanoparticulate in the gonadal region of a 61.4 µM ZnO NPs treated worms. **B,** TEM image of the gonadal region of a control worm with no observed nanoparticulate. **C,** TEM image of possible nanoparticulate under the cuticle region, black arrow indicates worm cuticle. **D,** Under higher magnification, possible nanoparticles were under the cuticle. *Nanoparticles were indicated by red arrows.

worm cuticles (Figure 3C). No similar images of possible NPs were observed in any areas of the control worms (Figure 3B). This indicates NPs could possibly be taken up through the worm cuticle and present in the gonadal region.

### *Apoptosis Assay*

SYTO 12 staining showed that ZnO NP treated wild-type N2 worms had an average of 1.6, 1.7, 4.6, and 2.8 apoptotic cells for the control, $6.14 \times 10^{-1}$, 61.4, and 614 µM treatment groups, respectively (Figure 4). Figure 5 shows the representative images of apoptosis observed following SYTO 12 staining in different groups. Although the $6.14 \times 10^{-1}$ µM group showed no significant difference compared with control, the 61.4 and 614 µM treatments significantly increased the number of apoptotic cells as compared with control. Interestingly, the number of apoptotic cells in the 61.4 µM ZnO NP treated group was significantly higher than the 614 µM treatment group ($P < .05$) (Figure 4). One the other side, $ZnCl_2$ treated worms had an average of 1.6, 1.6, 2.4, and 2.5 apoptotic cells for the control, $6.14 \times 10^{-1}$, 61.4, and 614 µM treatments, respectively (Figure 4). Although the $6.14 \times$

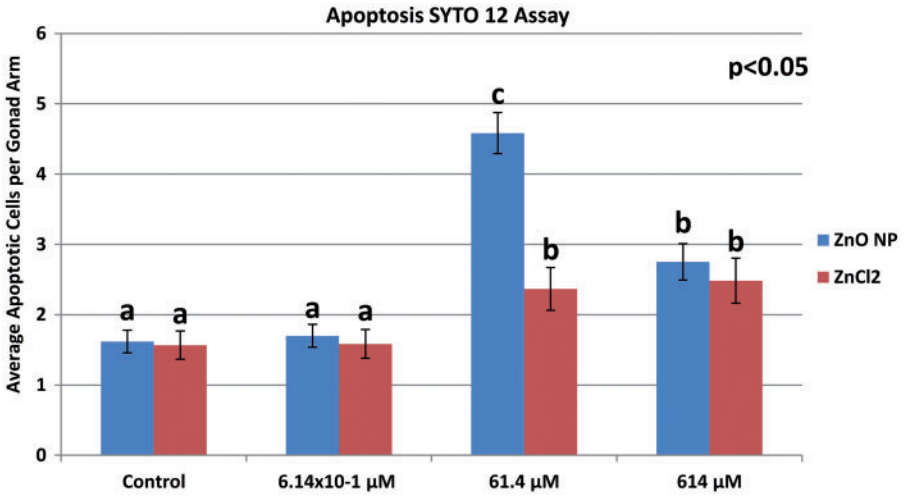


FIG. 4. Average number of apoptotic cells per gonad arm after L1-adult stage dosing for 72 h until adulthood. SYTO 12 staining of N2 strain. Different letters (a,b, and c) denote statistically significant different groups at $P < .05$ level; there were 3 statistical groups according to ANOVA "comparison of means" analysis, which were labelled as a, b, and c. Error bars indicate standard deviations of 3 individual experiments (each consisting of 10 worms).

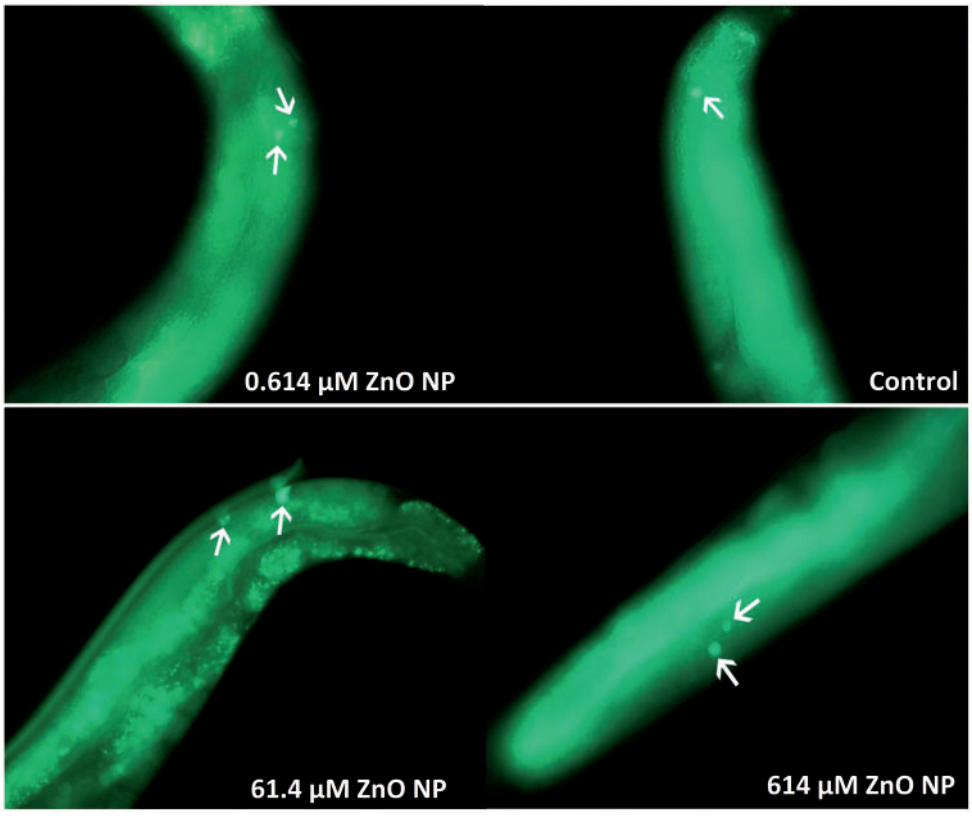


FIG. 5. Representative image of apoptotic cells following SYTO 12 staining observed in N2 strain under ZnO NP treatment for 72 h (from L1 to early adulthood). Apoptotic cells appear as solid green dots indicated by white arrows.

$10^{-1}$ µM $ZnCl_2$ treated group showed no significant difference compared with control, the 61.4 and 614 µM treatments significantly increased the number of apoptotic cells as compared with control ($P < .05$). Comparing the ZnO NP treatments to the $ZnCl_2$ treatments, no significant difference was found between the controls or the 614 µM treatment groups. However, apoptosis in the 61.4 µM ZnO treatment group was significantly higher than apoptosis in the 61.4 µM $ZnCl_2$ treatment group (Figure 4).

MD701 strain was used to further confirm the increased apoptosis under different treatments. ZnO NP exposed MD701 strain worms had an average of 1.5, 4.3, and 2.7 apoptotic cells for the control, 61.4 µM, and 614 µM treatments, respectively (Figure 7). Figure 8 shows the representative images of apoptosis observed in MD 701 strain subjected to different ZnO NP treatments. Both 61.4 and 614 µM ZnO NP treatments induced significantly more apoptotic germ cells than the control ($P < .05$). This was in consistent with findings using the N2 strain. Consistent

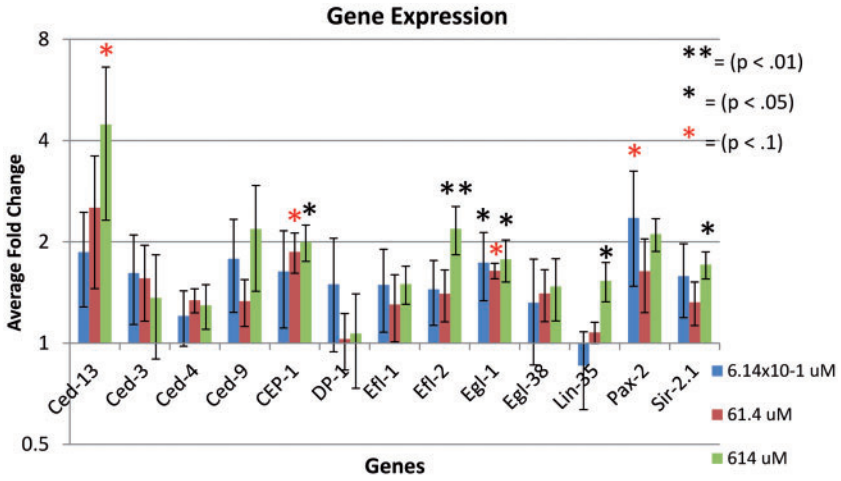


FIG. 6. Gene expression fold changes of the 13 tested genes in apoptosis pathway. All Ct values were normalized using Y45F10D.4 mRNA. The gene expression fold change were compared with a control value of 1 (>1 means up-regulated, <1means down-regulated). *Y-axis* uses a logarithmic scale with a base of 2 ($\log_2$). The error bars represent the standard error of fold change for 4 biological replicates per gene (n = 4).

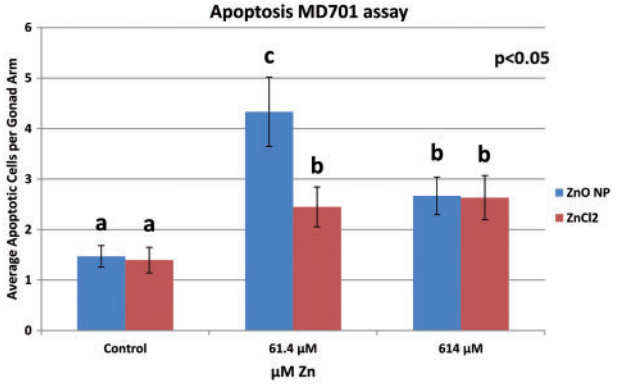


FIG. 7. The number of apoptotic cells per gonad arm observed in MD 701 (*bcIs39 [(lim-7)ced-1p::GFP + lin-15(+)]*) strain after L1-adulthood dosing for 72 h. Different letters (a,b, and c) denote statistically significant different groups at $P < .05$ level; there were 3 statistical groups according to ANOVA "comparison of means" analysis, which were labeled as a, b, and c. Error bars indicate SDs of 3 individual experiments (each consisting of 10 worms).

with what was observed using the N2 strain, the number of apoptotic cells in the 61.4 µM group was more than that of the 614 µM group ($P < .05$). On the other hand, $ZnCl_2$ treated worms had an average of 1.4, 2.5, and 2.6 apoptotic cells for control, 61.4 µM, and 614 µM treatments, respectively (Figure 7). Similarly to the ZnO NP treatments, both the 61.4 and 614 µM $ZnCl_2$ treated groups induced significantly more apoptotic cells than control ($P < .05$). In contrast to what was observed in the N2 strain, there was no difference in 61.4 and 614 µM $ZnCl_2$ treated groups. When comparing between ZnO NP and $ZnCl_2$ -induced apoptotic cells in the 61.4 µM treatment group, ZnO NP induced significantly more apoptosis than $ZnCl_2$ in this concentration (4.3 vs 2.6, $P < .05$, Figure 7).

To determine whether or not increased apoptosis induced by the ZnO NPs is *cep*-1/p53 dependent, treated TJ1strain was subjected to SYTO 12 staining. The TJ1 worms had averages of 1.6, 1.6, 2.0, and 1.7 apoptotic cells per gonad arm for the control, $6.14 \times 10^{-1}$, 61.4, and 614 µM ZnO NP treatments, respectively (Figure 9). Results showed no significant differences between control and treatment groups ($P > .05$).

*Gene Expression*

In general tested genes were upregulated following ZnO NP treatments, although the fold changes were small. Specifically *cep-1*, *efl-2*, *egl-1*, *lin-35*, and *sir-2.1* were significantly upregulated when treated with 614 µM of ZnO ($P < .05$) (Figure 6). In the $6.14 \times 10^{-1}$ µM treatment group, *egl-1* was significantly up-regulated ($P < .05$). The genes that showed significant upregulation with >2-fold expression changes were *cep-1*, *cep-13*, and *efl-2*. The upregulation of *cep-1* supports previous findings that the ZnO-induced apoptosis are likely *cep-1* dependent demonstrated by the TJ-1 assay. In addition, the upregulation of *efl-2* may promote apoptosis by enhancing the transcription of *ced-4* and *ced-3*, which initiates apoptosis.

## DISCUSSION

The hydrodynamic diameters of ZnO NPs were larger than those observed using TEM that has different sample preparation procedure. The reading from DLS measurement using Zetasizer is supposed to be larger than the SEM measurement; it measures the hydrodynamic diameter of the particles in suspension or solution. It uses the Stokes Einstein equation to calculate particle size that also takes into account the particle motion in liquid solution. Our measurements using SEM and Zetasizer were comparable with several independent labs's report that used the same instrument; previous studies have determined the average size of the ZnO NPs to be 20nm by TEM versus approximately 759 nm by DLS (Wang *et al.*, 2009) and 30 nm by TEM versus approximately 627 nm by DLS (Wu *et al.*, 2013). The hydrodynamic sizes represent the aggregated sizes of NPs in aqueous solutions that mimic its environmental existence forms. It is generally recognized that nanoparticles are stable and difficult to degrade, especially in our experiment where the exposure was conducted in the dark and lasted for only 72 h, thereby the photodegredation should be minimized. As dissolved free Zn from ZnO NPs is an important contributor to toxicity, it is necessary to estimate the dissolution rate. According to previous report where the dissolution rate of ZnO nanoparticle were studied extensively (Li *et al.*, 2013), the dissolution rate of ZnO under current experimental condition (pH = 6.8) was estimated as <15%, largely lower than the 100% free Zn ion in the $ZnCl_2$ solution.

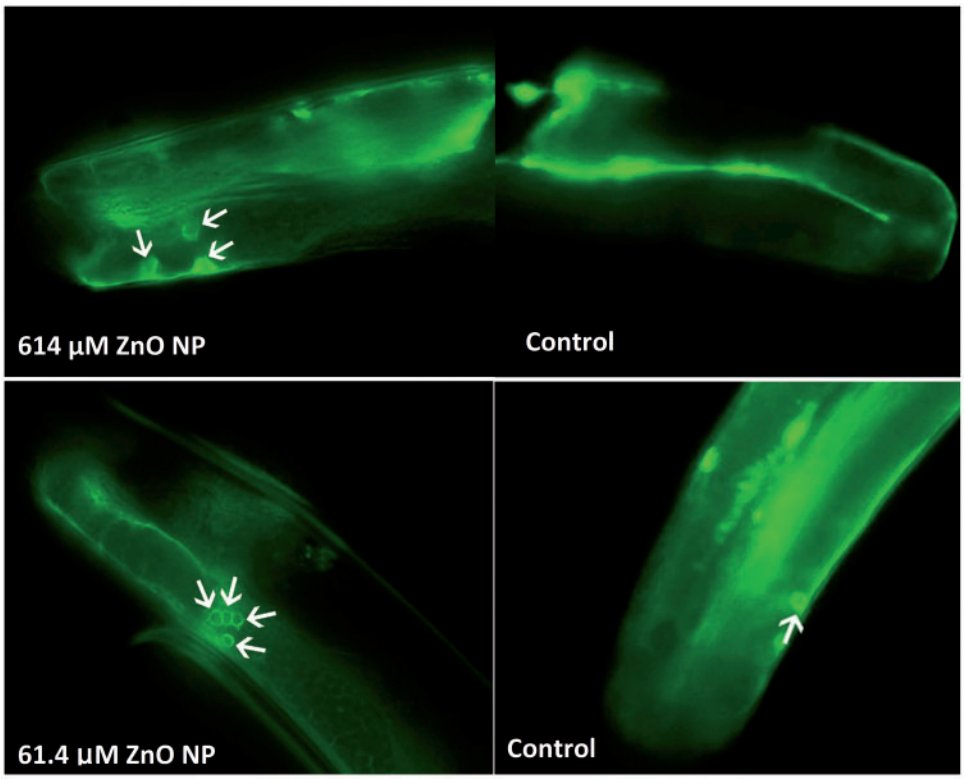


FIG. 8. Representative image of apoptotic cells observed in MD 701 (*bcIs39 [(lim-7)ced-1p::GFP + lin-15(+)]*) strain under ZnO NP treatment for 72 h (from L1 to early adulthood). Apoptotic cells appear as green fluorescent circles indicated by white arrows.

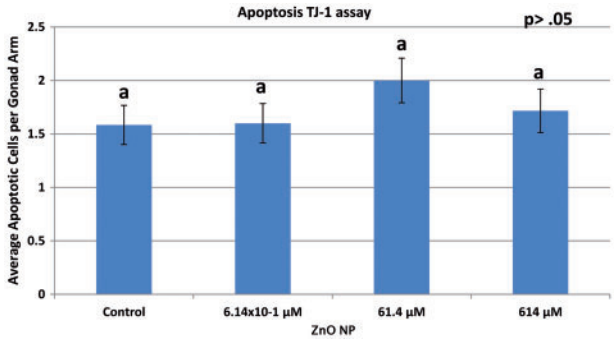


FIG. 9. The number of apoptotic cells per gonad arm observed in TJ1 (*cep-1(gk138) I*) strain after L1-adult dosing (72 h). The letter a denote there was no statistically significant differences among treatment groups at $P < .05$ level according to ANOVA "comparison of means" analysis. Error bars indicate SDs of 3 individual experiments (each consisting of 10 worms). No significant difference among control or any of the treatments.

Worms treated with ZnO NPs and vehicle control were sectioned to observe occurrence of NPs in vivo. Particulate-like objects was observed in ZnO NPs treated worms in both the gonad region as well the cuticle region. In contrast, no particulate-like objects were observed in any region of the control worms. This observation provides evidence that ZnO NPs may reach the gonadal region of the worm and thus they may interact with tissue components and contribute to the observed increases in germ cell apoptosis. The observations also suggested that one ZnO NPs uptake route is through the worm's cuticle. Future more study on the translocation of the ZnO NPs are needed.

The *C. elegans* germ cell apoptosis normally occurs in the transitional region (mitosis to meiosis) or the gonadal loop. As genetically unsuitable cells pass through the gonad loop or death zone they undergo apoptosis to prevent further maturation into oocytes (Hengartner 1997). Normally, in wild type *C. elegans* hermaphrodites, approximately 150 germ cells will undergo programmed cell death but only 0–3 corpses will be observed at any given time throughout the first 3–4 days of adulthood (Gumienny *et al.*, 1999). The apoptosis assays using N2 and MD701 strains all demonstrated that ZnO NPs and $ZnCl_2$ at concentrations of 61.4 and 614 µM promoted germ cell apoptosis. At 61.4 µM treatment group, ZnO NP induced significantly more apoptotic cells than $ZnCl_2$. This suggests that ZnO NPs are more efficient than ionic Zn to induce apoptosis at specific concentration. The TJ-1 (*cep-1*/p53 knock-out mutant) strain was used to determine if or not the increase in apoptosis caused by ZnO NPs was *cep-1*/p53 dependent. Since there was no significant increase in apoptosis among treatments and controls, the ZnO NP-induced apoptosis is likely through *cep-1*/p53-dependent pathway.

Interestingly, experiments in both wide-type N2 strain and the MD 701 strain all results in the similar findings that the 61.4 µM treatment yields more apoptotic cells than the 614 µM treatment. It is known that dose–response relationship is complex and many toxicants/drugs have multiphasic response due to different mechanisms such as feed-back inhibition, activation of other defense/detoxification mechanisms, etc. Specifically for apoptosis as a cellular response to stress, in some cases, is not a monophasic response. Such as in cancerous changes of healthy cells, apoptosis is inhibited under exposure to high concentrations of genotoxic, mutagenic, and carcinogenic agents. However, specific mechanism of this observation warrants future investigation.

To investigate the effects of ZnO NP on the expressions of genes involved in apoptosis, qRT-PCR analyses were performed.

In general the apoptosis pathway was activated by ZnO NP treatment and the observed increased apoptosis caused by ZnO NPs was not attributed to free $Zn^{2+}$ alone. Specifically, the *cep-1* was significantly up-regulated which supports that ZnO-induced germ cell apoptosis is through the *cep-1*/p53 dependent pathway. Apoptosis which is DNA damage related may show an up-regulation of the tumor suppressor cep-1/p53. The *egl-1*, *ced-13* genes were also up-regulated. EGL-1 and CED-13 interact directly with the anti-apoptotic CED-9, a homolog of mammalian BCL-2, and inhibit its transcription, inducing the release of CED-4 and consequently the activation of CED-3 (caspase) and result in apoptosis initiation (WormBase [http://www.wormbase.org/db/get?name=WBGene00000423;class=gene; http://www.wormbase.org/db/get?name=WBGene00001170;class=gene]). *Lin-35*, which was also up-regulated, encodes for Rb, the retinoblastoma protein, and promotes physiological apoptosis by inhibiting the transcription of *ced-9* (Gartner *et al.*, 2008). In addition, *efl-2* were up-regulated, *dpl-1* encodes for Dp (dimerization partner protein) in mammals and works along with *efl-2*, which encodes for the transcription factor E2F in mammals. DPL-1, Rb, and E2F likely work cooperatively to increase CED-4 and CED-3 expression, therefore promoting germ cell apoptosis (Gartner *et al.*, 2008).

Metal oxide NPs are poorly biodegradable and biological consequences of the exposure remain largely unknown (Wang *et al.*, 2009). Although many reports suggest nanoparticle exposure results in release of ROS, few studies have investigated nanoparticle-induced apoptosis, an effect that is highly correlated with oxidative stress. This study provides evidence that ZnO NP exposure promotes apoptosis in germ cells and the enhanced apoptosis effects was not fully attributed to ionic Zn. Finally this study also provides a mechanistic understanding of ZnO NPs-related reproductive toxicity.

## ACKNOWLEDGMENT

We would like to thank Dr Tom Fink for technical supports of TEM imaging.

## FUNDING

This work was supported by the faculty start-up fund of East Carolina University. This research was supported in part by NIEHS under award number P30ES025128.

## REFERENCES

Brenner, S. (1974). Genetics of Caenorhabditis-elegans. *Genetics* **77**, 71–94.

Consortium CeS (1998). Genome sequence of the nematode C-elegans: A platform for investigating biology. *Science* **282**, 2012–2018.

Cutter, A. D., Dey, A., and Murray, R. L. (2009). Evolution of the Caenorhabditis elegans Genome. *Mol. Biol. Evol.* **26**, 1199–1234.

Gartner, A., Boag, P. R., and Blackwell, T. K. (2008) Germline survival and apoptosis. WormBook, ed. The C. elegans Research Community, WormBook, Available at: http://www.wormbook.org/chapters/www_germlinesurvival/germlinesurvival.html. Accessed November, 2016.

Gumienny, T. L., Lambie, E., Hartwieg, E., Horvitz, H. R., and Hengartner, M. O. (1999). Genetic control of programmed cell death in the Caenorhabditis elegans hermaphrodite germline. *Development* **126**, 1011–1022.

Hengartner, M. O. (1997). Genetic control of programmed cell death and aging in the nematode Caenorhabditis elegans. *Exp. Gerontol.* **32**, 363–374.

Kaletta, T., and Hengartner, M. O. (2006). Finding function in novel targets: C-elegans as a model organism. *Nat. Rev. Drug Discov.* **5**, 387–398. doi:10.1038/nrd2031

Leung, M. C. K., Williams, P. L., Benedetto, A., *et al.*, (2008). Caenorhabditis elegans: An emerging model in biomedical and environmental toxicology. *Toxicol. Sci.* **106**, 5–28.

Li, M., Lin, D., and Zhu, L. (2013). Effects of water chemistry on the dissolution of ZnO nanoparticles and their toxicity to Escherichia coli. *Environ. Pollut.* **173**, 97–102.

Livak, K. J., and Schmittgen, T. D. (2001). Analysis of relative gene expression data using real-time quantitative PCR and the 2(T)(-Delta Delta C) method. *Methods* **25**, 402–408.

Ma, H., Bertsch, P. M., Glenn, T. C., Kabengi, N. J., and Williams, P. L. (2009). Toxicity of manufactured zinc oxide nanoparticles in the nematode Caenorhabditis elegans. *Environ. Toxicol. Chem.* **28**, 1324–1330.

Nel, A., Xia, T., Madler, L., and Li, N. (2006). Toxic potential of materials at the nanolevel. *Science* **311**, 622–627.

Polli, J. R., Zhang, Y., and Pan, X. (2014). Dispersed crude oil amplifies germ cell apoptosis in Caenorhabditis elegans, followed a CEP-1-dependent pathway. *Arch. Toxicol.* **88**, 543–551.

Ruan, Q.-L., Ju, J.-J., Li, Y.-H., *et al.*, (2012). Chlorpyrifos exposure reduces reproductive capacity owing to a damaging effect on gametogenesis in the nematode Caenorhabditis elegans. *J. Appl. Toxicol.* **32**, 527–535.

USEPA. U.S. Environmental Protection Agency. (2005). Nanotechnology and the Environment: Applications and Implications Progress Review Workshop III. Office of Research and Development, Washington, DC.

Wang, H., Wick, R. L., and Xing, B. (2009). Toxicity of nanoparticulate and bulk ZnO, Al2O3 and TiO2 to the nematode Caenorhabditis elegans. *Environ. Pollut.* **157**, 1171–1177.

Wu, Q., Nouara, A., Li, Y., *et al.*, (2013). Comparison of toxicities from three metal oxide nanoparticles at environmental relevant concentrations in nematode Caenorhabditis elegans. *Chemosphere* **90**, 1123–1131.